Available online at www.sciencedirect.com
ScienceDirect
Journal of Electron Spectroscopy and Related Phenomena 156–158 (2007) 387–392
JOURNAL OF ELECTRON SPECTROSCOPY and Related Phenomena
www.elsevier.com/locate/elspec

Electron inelastic mean free path in solids as determined by electron Rutherford back-scattering

M.R. Went [a,*], M. Vos [a], R.G. Elliman [b]

[a] *Atomic and Molecular Physics Laboratories, Research School of Physical Sciences and Engineering, The Australian National University, Canberra, ACT 0200, Australia*
[b] *Electronic Materials Engineering, Research School of Physical Sciences and Engineering, The Australian National University, Canberra, ACT 0200, Australia*

Available online 30 November 2006

Abstract

Energetic electrons scattering elastically over large angles from atoms lose energy depending on the mass of the scattering atom. If the energy of the incident electron is large enough, 10's of keV, this energy loss can be measured with high resolution electron spectrometers, allowing the separation of heavy and light elements. This technique is in many ways analogous to Rutherford back-scattering (RBS), with electrons employed as the scattering particle rather than ions. We refer to these measurements as electron Rutherford back-scattering (ERBS). We present ERBS data for a simple two-layer system (gold on carbon). It is shown that this method can be used to determine the inelastic mean free path of electrons in carbon. We obtain a value of 350 ± 50 Å for 40 keV electrons in amorphous carbon. A comparison of the ERBS results is made with traditional RBS results from the same film. A consistent interpretation of both measurements using calculated differential elastic cross sections was not obtained.

Keywords: Elastic scattering; Thin film analysis; Inelastic mean free path

1. Introduction

With recent improvements in the resolution of high energy electron spectrometers it has become feasible to examine details of elastic scattering from solids. When an electron is scattered from a target with high momentum transfer, momentum, and hence energy is transferred from the incident electron to the nucleus of the target atom. The associated energy loss is dependant on both the momentum transfer and the mass of the scattering atom. For sufficiently high resolution spectrometers this energy loss can be used to separate the contribution of different elements.

The energy loss for scattering from a stationary target of mass M at a momentum transfer of $\mathbf{q}$ is simply the recoil energy of the target atom: $E_r = \mathbf{q}^2/2M$. More realistically (even at 0 K there is the zero point motion of atoms in a lattice) the target atom will have an initial momentum $\mathbf{k}$ and in this case the recoil energy is given by the relation

$$E_r = \frac{(\mathbf{k}+\mathbf{q})^2}{2M} - \frac{k^2}{2M} = \frac{q^2}{2M} + \frac{\mathbf{q}\cdot\mathbf{k}}{M} \quad (1)$$

The first term in the above relation describes the shift of the elastic peak for targets of different mass, with heavier elements being shifted less than lighter ones. The second term is a Doppler broadening term and introduces a shift depending on the momentum of the target atoms relative to the momentum transfer direction. This broadening has been observed previously for both electron [1,2] and neutron [3] scattering from carbon.

If nuclei with very different masses are present in the target then the elastic peaks from each element will appear as separate peaks at slightly different energies. This was recently demonstrated for the case of a two layer system containing carbon and germanium [4]. Interpretation of the intensities proved to be difficult and was somewhat affected by poor sample preparation. Here we repeat this experiment at higher energies (larger element separation) for the C/Au system. These are free standing targets and measurements can be done both in transmission and reflection. Due to the large atomic number the elastic cross section of Au is much larger than for carbon. The targets were prepared in

* Corresponding author. Tel.: +61 2 6125 2705; fax: +61 2 6125 2452.
E-mail address: michael.went@anu.edu.au (M.R. Went).

0368-2048/$ – see front matter © 2006 Elsevier B.V. All rights reserved.
doi:10.1016/j.elspec.2006.11.041

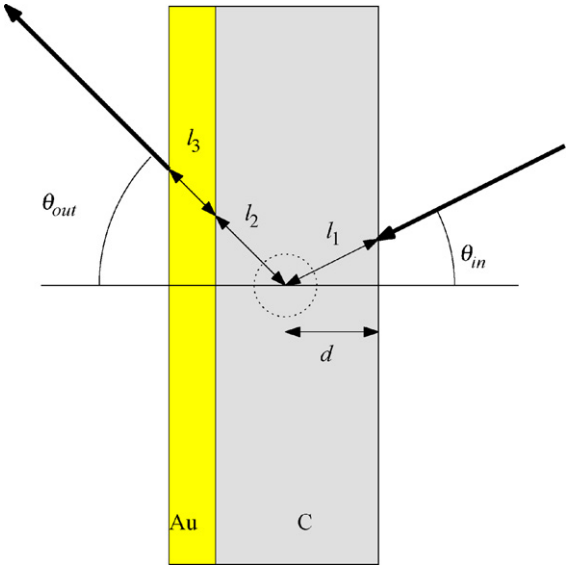

Fig. 1. Sketch of the experimental geometry showing the path length of the trajectories.

such a way that the signal from Au and C are comparable, hence the Au layer was much thinner than the carbon layer.

In the absence of inelastic loss processes, the ratio of the elastic peak areas is given simply by $(A_1/A_2) = (N_1\sigma_1/N_2\sigma_2)$, where $N_{1,2}$ and $\sigma_{1,2}$ are the number of atoms per unit area of element 1,2 and their respective differential elastic cross sections. In reality, even for very thin films, inelastic scattering has a large effect on the observed intensities. Electrons which have undergone an inelastic collision do not contribute to the elastic peak but are observed at much lower energies. Fig. 1 shows a schematic diagram of the experiment in the 'single scattering approximation' used throughout this work. The fraction of electrons passing, without energy loss, through a material with inelastic mean free path (IMFP) λ are attenuated as they travel through length l of material such that

$$I = I_0\, e^{-(l/\lambda)}. \tag{2}$$

Elastic scattering occurs at a rate proportional to $\rho\sigma$, where ρ is the atomic density and σ is the differential elastic cross section. Thus for the event depicted in Fig. 1 the contribution to the signal from in the elastic peak from depth d is given by,

$$I = I_0\rho_1\sigma_1\, e^{-(l_1/\lambda_1)}\, e^{-(l_2/\lambda_1)}\, e^{-(l_3/\lambda_2)}. \tag{3}$$

By integrating the signal over layer 1 we get the intensity of peak 1. Integrating an equivalent equation over layer 2 gives the intensity of peak 2. The ratio of the two signals, obtained in this way, can be compared to the experimental one. In the cases studied here, the Au layer thickness (a few Å) is much smaller than its IMFP (a value of 246 Å, obtained from the TPP-2M method [5], was used in this work), hence the outcome of Eq. (3) does not depend critically on the mean free path assumed for Au. $\sigma_{1,2}$ are

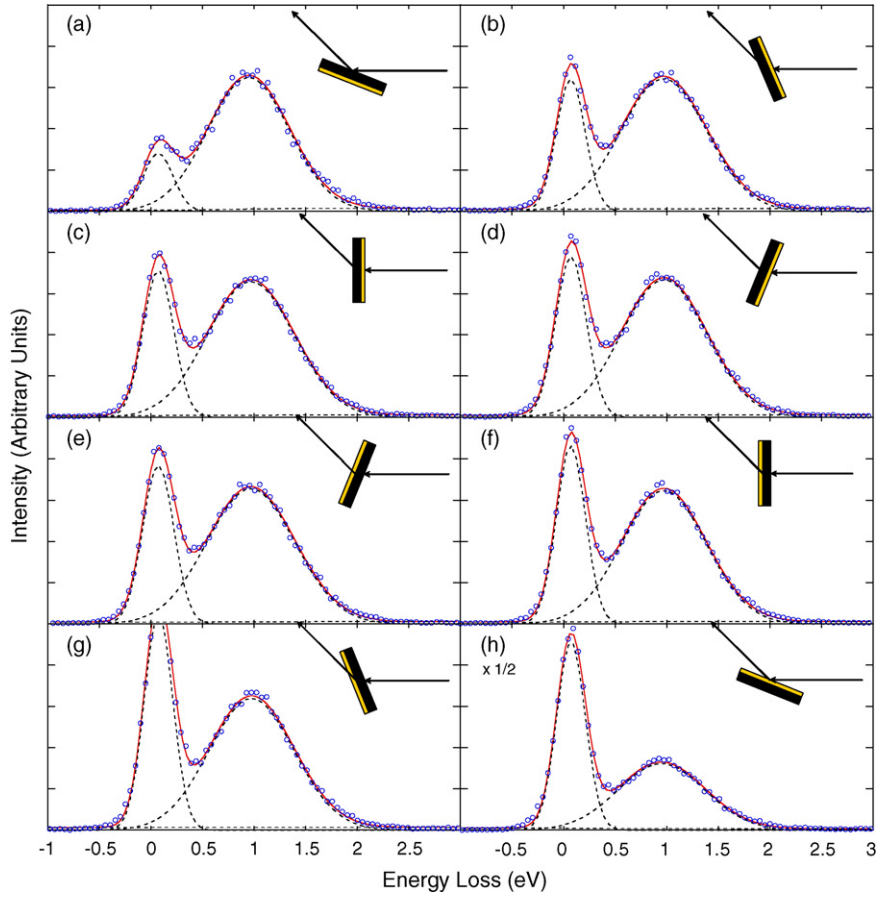

Fig. 2. Measured ERBS spectra for a 90 Å carbon foil with 1 Å of Au deposited.

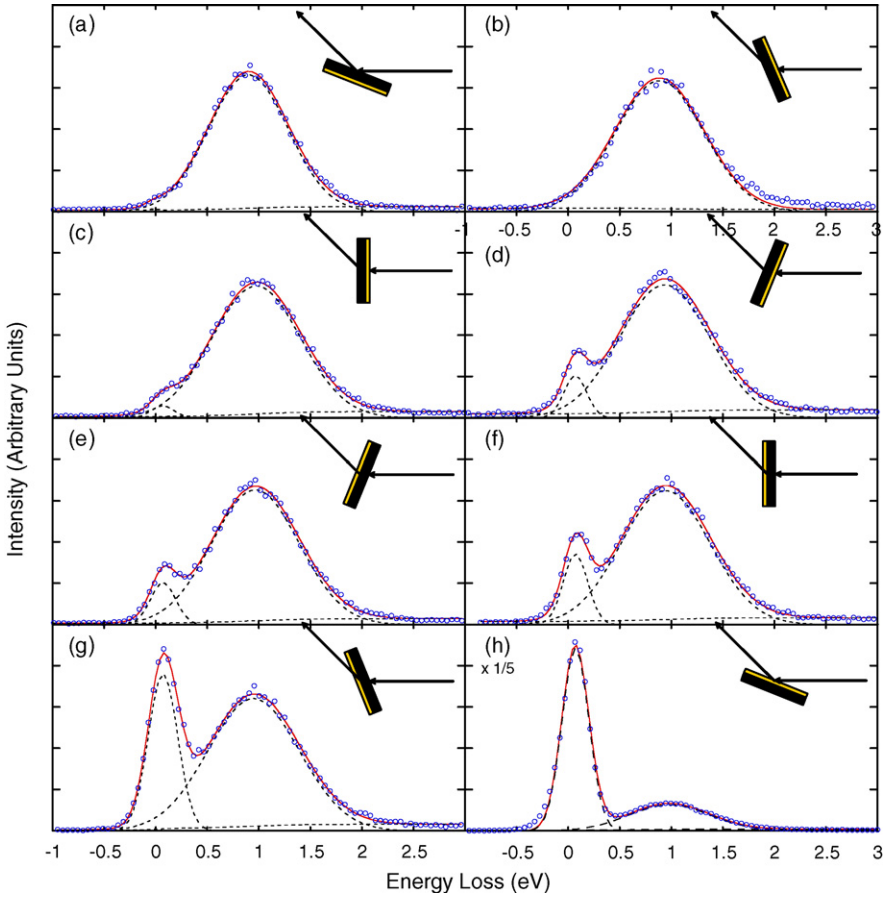

Fig. 3. Measured ERBS spectra for a 1400 Å carbon foil with 2 Å of Au deposited.

known (at 40 keV, we obtained, using the ELSEPA program [6], for scattering over 44.6° a value of 1.45×10^{-21} cm^2/sr for C and 1.77×10^{-19} cm^2/sr for Au). Note that the calculated cross sections of Au and C do not scale like Z^2 as would be expected for Rutherford like cross-sections. This is an indication that for Au screening of the nuclear charge by inner shell electrons is significant for the scattering conditions described here.

In Figs. 2 and 3 the different geometries measured in this work are shown. The two reflection geometries (a) and (h) are the most surface sensitive. For geometries (d) and (e) $\theta_{in} = \theta_{out}$ and hence the path length (for either layers 1 or 2) is independent of the depth at which the elastic scattering occurs. The attenuation of the signal of layer 1 is thus the same as the attenuation of layer 2 and the ratio of both signal intensities is thus independent of either IMFP. These two geometries should produce identical ERBS spectra and the peak area ratio should be described by $(A_1/A_2) = (N_1\sigma_1/N_2\sigma_2)$. Subsequently, using the known thickness of the carbon film any of the remaining spectra can be used to find the IMFP of carbon. As six additional, different geometries are measured the spread in the outcome for each of these geometries gives an indication of the accuracy of the method.

The standard method for determining the IMFP is the so called elastic peak electron spectroscopy (EPES) [7,8] where it is assumed that elastic scattering is well understood and any reduction in the elastic peak size is due to electrons having been inelastically scattered. Current measurements and calculations [5,9] on the IMFP of electrons in matter are largely focused at XPS energies in the ≈ 1 keV range, extrapolating to the 10's of keV range is stretching the limits of the original data. A method by which the IMFP can be determined in this energy range is desirable and will allow improvements on the current models.

2. Experiment

The apparatus used for these measurements has been described previously [4,10]. Recent developments have focussed on increasing the energy of the incoming beam and improving the analyzer resolution so that ERBS measurements from a suitable two element system show well resolved peaks. An electron gun produces a beam of 500 eV electrons by thermionic emission from a heated BaO surface. These electrons are accelerated to 40 keV where they are incident on the sample which is maintained at that potential. The electron beam at the sample position is ≈ 0.1 mm in diameter. Electrons either pass through the sample and are collected in a Faraday cup behind the sample or are scattered inside the material. Electrons which are scattered through 44.6° pass through an aperture, are decelerated to 200 eV and are focused, using slit lenses, onto the entrance of the electron energy spectrometer. The electrons which pass through the spectrometer are detected by a 2D position sensitive detector. This configuration allows the simultaneous col-

lection of electrons within an energy range ≈ 40 eV and over a 13° azimuthal angular range. The sample is mounted such that it can be rotated through 360° and all measurement geometries shown in Figs. 2 and 3 can be accessed for the same sample.

The samples consist of various thicknesses of amorphous carbon foils (90, 350, 700 and 1400 Å)(supplied by Arizona Carbon Foil Company) which are mounted over 2 mm diameter holes in a 0.1 mm thick stainless steel shim. These holes allow the electron beam to pass through the foil without scattering from the shim for a large range of incident angles. First the carbon films are heated by electron bombardment into the 350–600 °C range. This serves to increase conductivity and remove weakly bonded contaminants. Subsequently, it was checked that the elastic peak consisted of a single component by performing an ERBS measurement. Next gold is evaporated onto the foils by resistive heating of a tungsten basket containing gold wire. The deposition rate of gold in monitored concurrently by a vibrating quartz crystal thickness monitor. This is used as a rough indication only, as the amount of Au deposited is close to the lower limit the crystal balance can resolve. After deposition the samples are returned (under vacuum) to the spectrometer. The pressure in the preparation chamber is $< 10^{-8}$ Torr while evaporation is performed. The pressure in the measurement chamber is maintained at $< 10^{-10}$ Torr ensuring that contamination is minimized. It is likely that the gold deposited onto the carbon films forms islands, 100% coverage is not achieved until ≈ 60 Å (3.7×10^{16} atoms cm^{-2}) have been deposited [11]. This does not reduce the validity of the single scattering approach as the height of the islands is significantly less than the IMFP, hence attenuation effects are insignificant. The method is also insensitive to the layer morphology as the island coverage is averaged over the area of electron beam.

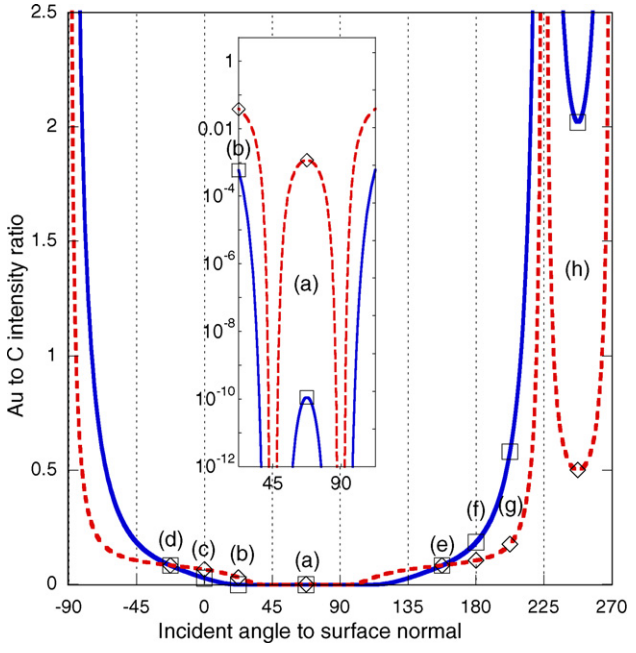

Fig. 4. Calculations of peak intensity ratios for two film thicknesses (1400 Å C with 2.1 Å Au: solid line; 350 Å C with 0.5 Å Au: dashed line). The various geometries (a–h) as indicated in Figs. 2 and 3 are labeled. The angle given is the angle between the incident beam and the carbon surface normal. Insert shows the area around 67.5° on a log scale.

For each sample, measurements are made in the eight geometries shown in Figs. 2 and 3. After the ERBS measurements are completed the samples are transferred out of the vacuum and are prepared for measurement by conventional RBS. This involves mounting the free standing films and support shim over a Faraday cup. The RBS measurements were performed with a 2 MeV He^+ beam. This beam has a larger diameter than the electron beam (about 1 mm) and some scattering from the support shim was observed. However the carbon and Au peaks were clearly resolved, and their areas were determined in a straightforward manner. Analysis was undertaken using the RUMP package. For the ions the scattering cross section scaled in good approximation as Z^2.

3. Results and discussion

In Figs. 2 and 3 the ERBS spectra are presented for each of the eight geometries for the two extreme carbon thicknesses. The leftmost peak centered at 0.07 eV is due to scattering from Au while the second peak which is centered near 1 eV is due to scattering from carbon. The width of the Au peak is assumed to be the experimental resolution, the much larger width of the carbon peak is due to Doppler broadening. The intensities of the two peaks are determined by fitting of the measured spectra with two Gaussian peaks. Each peak has three free fitting parameters (area, position and width). Under the elastic peak a very small background develops, due to inelastic scattering with very small energy losses. This is modelled by a Shirley background [12] which introduces an additional independent fitting parameter. The observed peak intensity ratio is compared with that obtained from evaluating Eq. (3).

First, consider the spectra for geometry (d) and (e). Here the mean free path should not affect the ratio of the observed peaks and we expect both spectra to be identical (see Fig. 4). Indeed experimentally this appears to be the case. Using the calculated elastic scattering cross section we can determine the atomic ratio ($N_C : N_{Au}$) by ERBS and compare this the results obtained by RBS. This is done in Table 1. There seems to be a systematic difference of ≈ 30% between the results obtained by the two methods. As the measurements ERBS (in geometries (d) and (e)) and RBS are independent of the IMFP and stopping power, respectively, the source of this difference can only be attributed to the cross sections. If multiple scattering is the cause

Table 1
Atomic ratios determined by ERBS and RBS for each sample measured

Sample	$N_C : N_{Au}$		
	ERBS (10%)	RBS (10%)	Ratio
90 Å C + 1 Å Au	295		
350 Å C + 0.5 Å Au	1710	1280	0.74
700 Å C + 1 Å Au	1640	1020	0.62
1400 Å C + 2 Å Au	1460	1050	0.71

The ratio of the RBS to ERBS measurement is also given. Calculation of ERBS intensity ratios for different incident beam angle. Estimated errors due to the peak decomposition are shown in parentheses.

Table 2
Peak area ratios measured and calculated

Geometry	Au/C peak area ratio		
	Measured	Calculated (IMFP 605 Å)	Calculated (IMFP 350 Å)
90 Å carbon + 0.65 Å Au			
(a)	0.16	0.28	0.19
(b)	0.33	0.36	0.33
(c)	0.38	0.40	0.39
(d)	0.41	0.41	0.41
(e)	0.42	0.41	0.41
(f)	0.46	0.43	0.44
(g)	0.55	0.47	0.51
(h)	0.9	0.8	0.9
350 Å carbon + 0.45 Å Au			
(a)	0.00	0.01	0.00
(b)	0.03	0.04	0.03
(c)	0.05	0.06	0.06
(d)	0.08	0.07	0.07
(e)	0.07	0.07	0.07
(f)	0.09	0.08	0.09
(g)	0.15	0.11	0.15
(h)	0.47	0.28	0.47
700 Å carbon + 0.95 Å Au			
(a)	0.00	0.00	0.00
(b)	0.01	0.02	0.01
(c)	0.07	0.06	0.04
(d)	0.07	0.08	0.08
(e)	0.08	0.08	0.08
(f)	0.13	0.10	0.11
(g)	0.61	0.18	0.27
(h)	1.0	1.8	0.9
1400 Å carbon + 2.1 Å Au			
(a)	0.00	0.00	0.00
(b)	0.00	0.00	0.00
(c)	0.02	0.05	0.03
(d)	0.09	0.08	0.08
(e)	0.08	0.08	0.08
(f)	0.15	0.13	0.19
(g)	0.38	0.35	0.58
(h)	2.3	1.2	2.0

Calculation are based on the indicated Au thickness and an IMFP of 350 Å for carbon.

of the discrepancy one would expect to see an increase in the deviation with increasing carbon thickness. The cross sections used in RBS are well established and it is difficult to see how such a large error can be attributed to these. This deviation is also larger than the changes which can be attributed to input choices of the "ELSEPA" program [6,13]. The origin of this discrepancy is thus unclear.

Using the nominal thickness of the carbon film and the ratio $N_C : N_{Au}$ determined for geometry (d) and (e) we can calculate the intensity ratio for the other geometries. In these other geometries we are sensitive to the value of the IMFP. Using the value of 605 Å obtained by extrapolating the TPP-2M formula to the current energy of 40 keV (well outside the range the TPP-2M formula claims to describe) we obtain poor agreement between experiment and calculation (see Table 2). Clearly the attenuation effects are underestimated using this value of the IMFP. By trial and error it was established that a much better fit of the experimental ratios is obtained using a value of 350 ± 50 Å for the 350 Å carbon film. The simpler Bethe equation [9] performs considerably better, predicting 405 Å for the IMFP.

This empirically determined value for the IMFP was used for all remaining sample thicknesses. The results of the calculations and the relative peak area measurements for the four samples and eight geometries are presented in Table 2. Only for the thinnest films is the Au observable in the reflection from the carbon side (geometry (a)) this is demonstrated in Fig. 4(insert), films that are thicker than about half the mean free path attenuate the gold signal to the point where it becomes undetectable. For most measurements good agreement can be seen when compared to the calculations ($\lambda = 350$ Å). The discrepancy for geometry (g) for the two thickest films can be explained by examining the topology of the calculations shown in Fig. 4. For measurements in the vicinity of the asymptotes (where the incoming or outgoing beam runs parallel to the surface) small variations in the surface normal due to film warping or misalignment cause significant shifts in the intensity ratio. For an identical Au to C ratio but for a thinner carbon film this problem is reduced considerably by the smaller gradient. Differences between the assumed Gaussian peak shape also start to affect the quality of the peak decomposition for larger Au peak intensities, particularly for the Au peak where the small natural width is broadened by the thermal distribution of the electron beam causing a Maxwell–Boltzmann type distribution. Recent measurements have also shown that the carbon elastic peak has an asymmetric shape caused by final state effects of the carbon in the lattice [4,14].

4. Conclusions

Electron Rutherford backscattering ERBS has been demonstrated as a alternate way by which the IMFP in matter can be determined. If the measurements are performed in specific geometries then the thickness of a deposited layer can be determined independent of the IMFP if differential cross sections are know to sufficient accuracy. Alternatively if the film thickness can be determined by alternate means, e.g. RBS, then ERBS can be used to determine relative differential cross sections.

Current extensions on this method will increase the momentum transfer 2.5× which will result in a sixfold increase in the peak separation. With the current experimental resolution this will allow the separation of three or more elements. Improvements to the method by which the RBS measurements are made by mounting the samples on a solid backing will also reduce errors and allow a better comparison between the two methods. In this way RBS should be able to give us not only the ratio of the number of atoms present but also the absolute number. Then the thickness of the carbon film can be verified as well, hopefully pinpointing the source of the 30% discrepancy.

Acknowledgements

The authors wish to acknowledge the useful discussions with W.M. Werner. This work is made possible by a grant of the Australian Research Council.

References

[1] H. Boersch, R. Wolter, H. Schoenebeck, Z. Phys. 199 (1967) 124.
[2] M. Vos, Phys. Rev. A 65 (2002) 12703.
[3] A. Fielding, D. Timms, J. Mayers, Europhys. Lett. 44 (1998) 255.
[4] M. Went, M. Vos, Surf. Sci. 600 (2006) 2070.
[5] S. Tanuma, C. Powell, D. Penn, Surf. Interf. Anal. 20 (1993) 77.
[6] F. Salvat, A. Jablonski, C. Powell, Comput. Phys. Commun. 165 (2005) 157.
[7] W. Werner, T. Cabela, J. Zemek, P. Jiricek, Surf. Sci. 470 (2001) 325.
[8] W. Werner, C. Tomatik, T. Cabela, G. Richter, H. Störi, J. Electron Spectrosc. Relat. Phenom. 113 (2001) 127.
[9] T. Malis, S. Cheng, R. Egerton, J. Electron Micros. Technol. 8 (1988) 193.
[10] M. Vos, G.P. Cornish, E. Weigold, Rev. Sci. Inst. 71 (2000) 3831.
[11] C. Templier, S. Muzard, A. Galdikas, L. Pranevicius, J. Delafond, J. Desoyer, Surf. Coat. Technol. 125 (2000) 129.
[12] D.A. Shirley, J. Phys. B: At. Mol. Phys. 5 (1972) 4709.
[13] A. Jablonski, F. Salvat, C. Powell, Surf. Interf. Anal. 37 (2005) 1115.
[14] M. Vos, M. Went, Phys. Rev. B 74 (2006) 205407.